Electronic Supplementary Material (ESI) for Environmental Science: Water Research & Technology.

Electronic Supplementary Information for:

Upcycling of plastic membrane industrial scraps and reuse as sorbent for emerging contaminants in water

Contents:

1. Molecular structure of selected contaminants

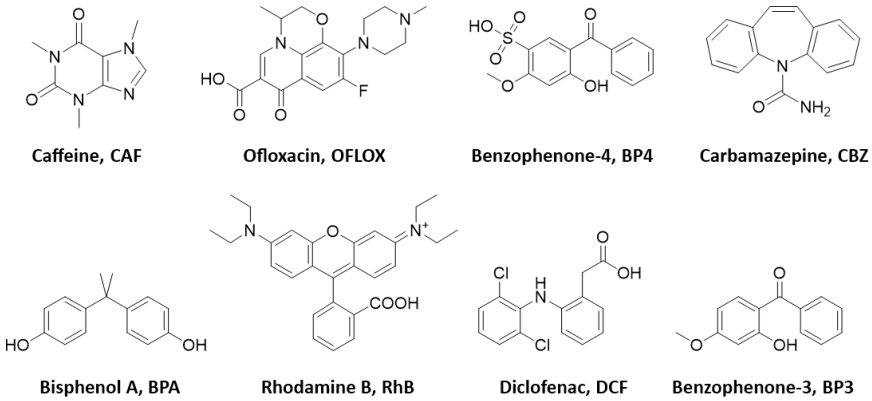

Fig. S1. Molecular structure of selected organic contaminants.

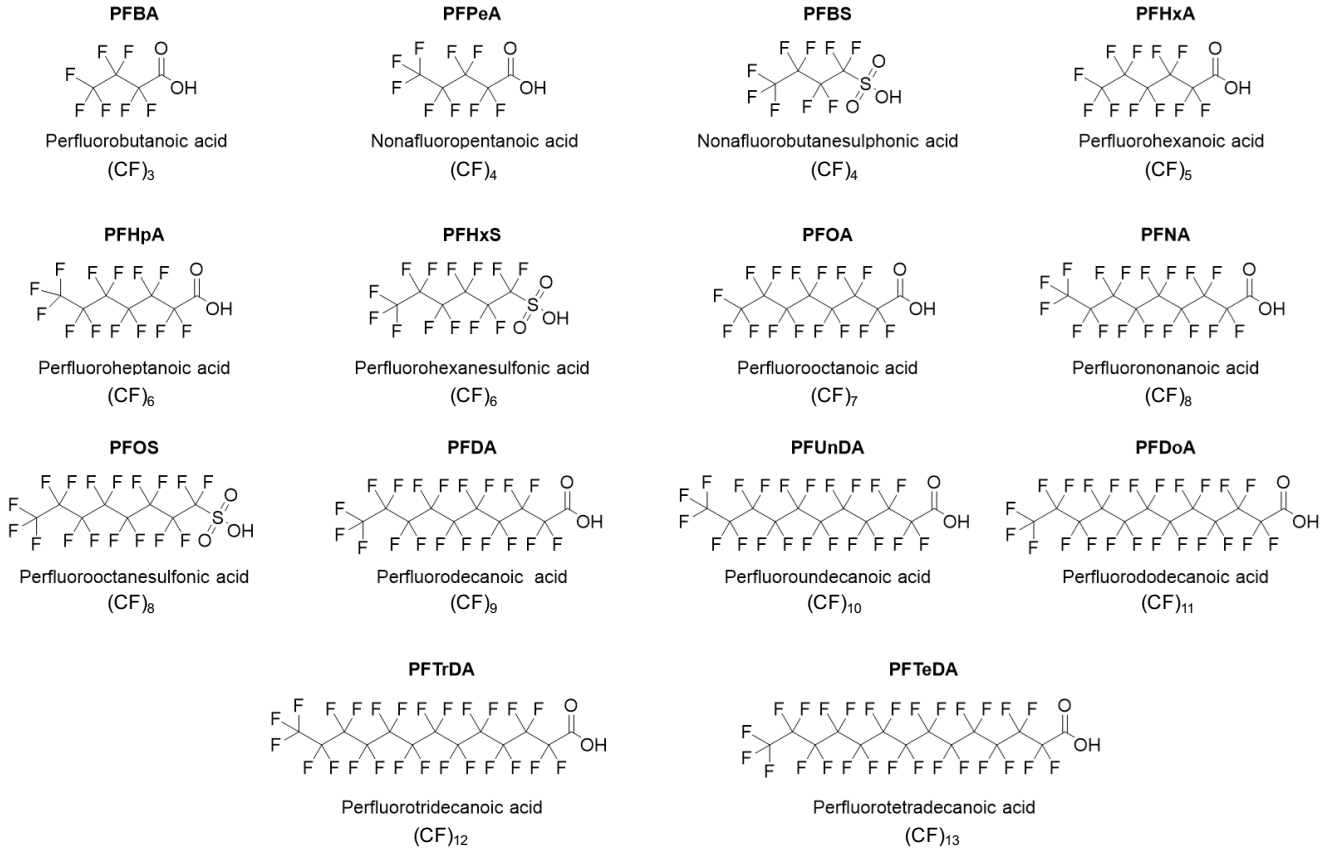

Fig. S2. Molecular structure of selected PFAS.

2. GAC technical data

Table S1. Technical details of GAC purchased from CABOT Norit Spa (Ravenna, IT, Norit GAC 830 AF). NORIT GAC 830 is a granular activated carbon produced by steam activation of select grades of coal.

Specifications	
Iodine number *(ASTM D 4607, 2014)*	> 1000 mg/g
Methylene blue index *(MU 182:98 M35)*	> 240 mg/g
Water soluble ashes *(MU 182:98 M33)*	< 11%
Granulometry >8 US mesh *(MU 182:98 M32)*	< 5 %
Granulometry <30 US mesh *(MU 182:98 M32)*	< 5%
Moisture (as packed)	< 5%
Ball-pan hardness *(ASTM D 3802)*	> 90
Apparent density *(MU 182:98 M31)*	> 450 kg/m^3
Molasses index *(Norit Standard Test Method)*	> 230
Pores distribution	Micro: > 45%; Meso: > 30%
Total pores volume	0.9-1.1 mL/g
Surface area *(BET method)*	> 1000 m^2/g
Uniformity coefficient	> 1.9
Density backwashed and drained	> 400 kg/m^3
Bed expansion	> 8% at linear rate 12.5 m/h at 20 °C

3. Materials and cartridge preparation

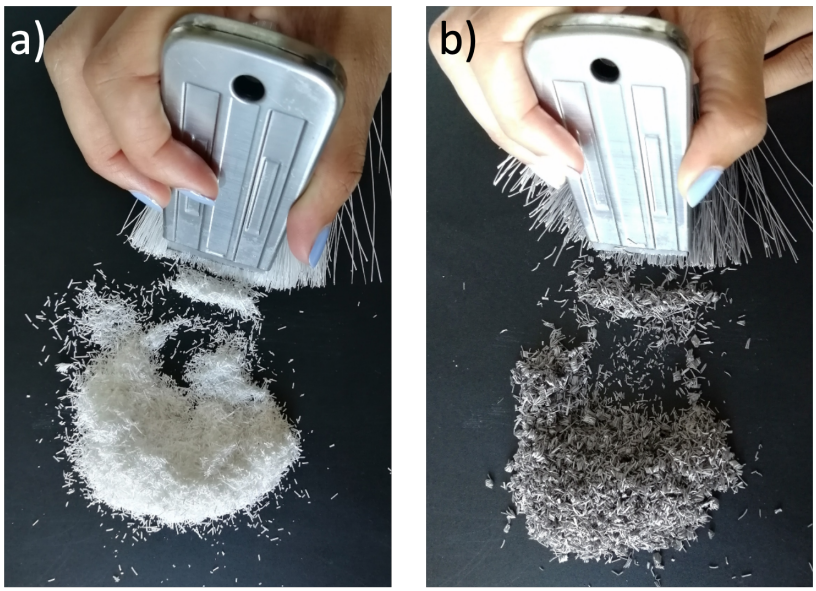

Fig. S3. Manual grinding PSU (a) and PSU-GO (b).

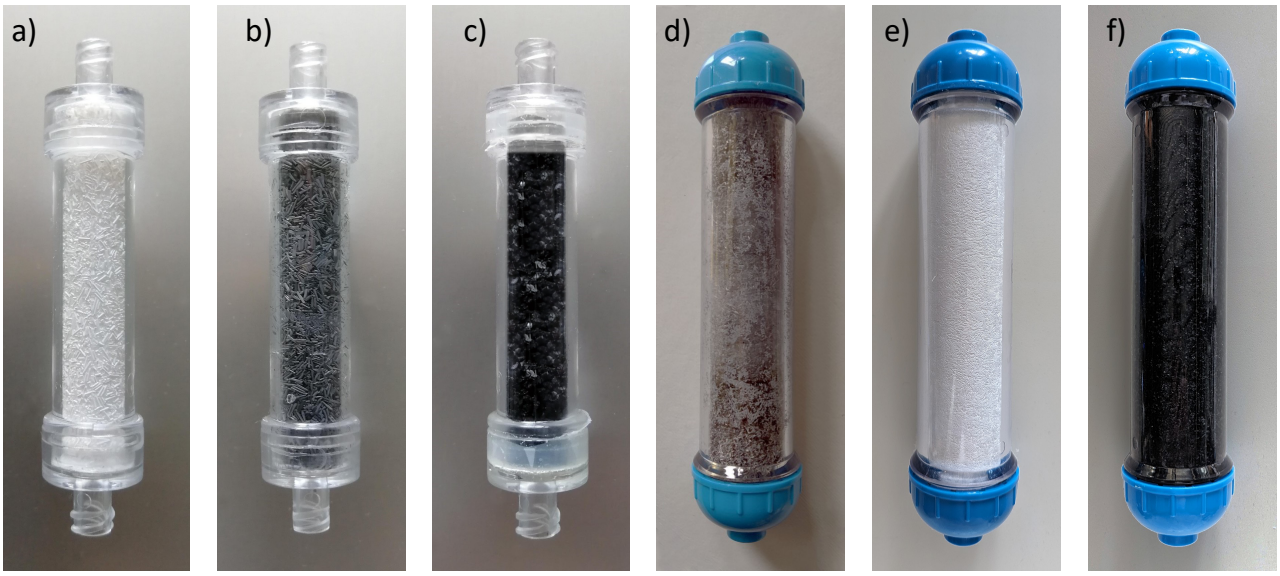

Fig. S4. Cartridge filled with granules: a) PSU (0.4 g), b) PSU-GO (0.73 g), c) GAC (2.3 g), d) PSU-GO granules (33 g), e) PSU granules (33 g),f) GAC (130 g). a) – c) Small cartridge (mm 14 x 65, EBCT = 0.5 min, Bed volume= 0.01 L), d-f) commercial standard size cartridge (mm 49 x 250, EBCT = 0.14 min, Bed volume 0.5 L).

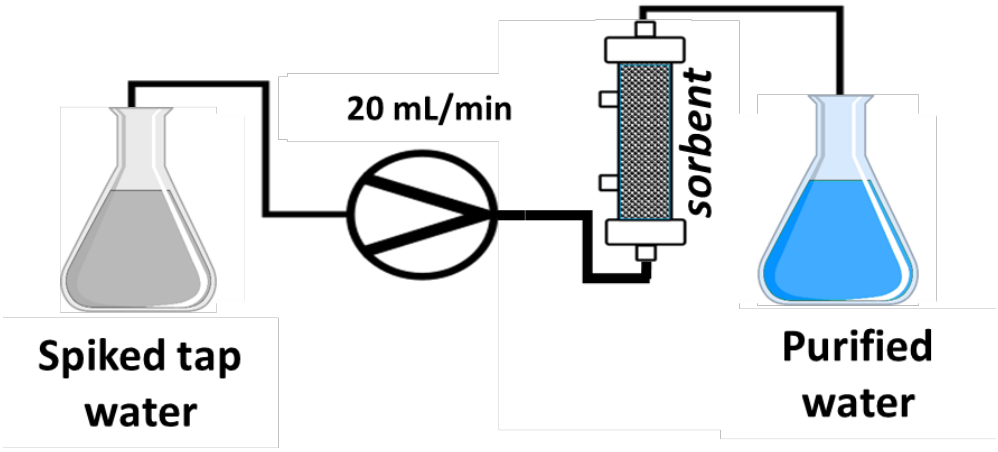

Fig. S5. Scheme of the experimental set up used for the experiments. The spiked solution flowed through the cartridge and the purified water was analysed. Flow rate: 20 mL/min, EBCT = 0.5 min. The same set-up was used to wash the cartridge before use, to remove glycerine. In this case, ultrapure water was filtered through the cartridge.

4. Experimental conditions for quantification of contaminants in water

4.1. ICP-MS method for heavy metals analysis

All the determinations were carried out with inductively coupled plasma triple quadrupole mass spectrometry (ICP-MS). A PerkinElmer NexION 1˙000 instrument was used for the analysis of the mixture of eight heavy metals and metalloids, and for loading curve experiments of lead. The operating conditions are listed below: nebulizer gas flow rates: 0.94 L/min; auxiliary gas flow: 1.2 L/min; plasma gas flow: 15 L/min; ICP RF power: 1˙600 W. Detection limit=1 µg/L.

4.2. HPLC-UV for organic contaminants analysis

HPLC analyses of the selected emerging contaminants in mixture were performed on a Dyonex Ultimate 3˙000 system equipped with a diode array detector. 0.5 mL samples were used as sources for the automated injection. The chromatographic separation was performed on a reverse phase Zorbax XDB-C8 column (4.6 × 150 mm, 5 µm) at flow rate of 1.0 mL/min, detection at λ_{max} of each analyte, linear gradient TFA 0.05% aqueous solution/acetonitrile from 80:20 to 0:100. In every experiment, the removal of each analyte was determined by comparison with that of the initial untreated solution. The results are expressed as the mean of three independent experiments ± SD. Detection limit=0.05 mg/L.

4.3. UPLC-MS/MS method for PFAS analysis

UPLC-MS/MS analyses on PFAS were performed by using an UPLC-MS/MS Waters ACQUITY UPLC H-Class PLUS – XEVO TQS Micro mass detector. The chromatographic separation was performed on a reverse phase Waters Acquity UPLC CSH Phenyl-Hexyl (1.7µm, 2.1 x 100 mm) column and Waters Isolator Column (2.1 x 50 mm). The column temperature was 34 °C, the flow rate 0.3 mL/min and the injection volume 40 µL, while the total run time was 21 minutes for PFAS and 11 minutes for PFOA analyses. The mobile phase consists of a biphasic gradient, NH_4OAc 2 mM in a mixture of ultrapure water:methanol 95:5 as phase A, and NH_4OAc 2 mM in MeOH as phase B. The mobile phase composition varied according to the gradient program reported in Table S2 for PFAS and in Table S3 for PFOA analyses. Mass details and the transitions monitored for each analyte are reported in Table S4. The calibration curves were calculated by using the average value of 2 subsequent UPLC-MS/MS injections. Calibration curve solutions (0.01, 0.05, 0.1, 0.5, 1, 2.5 µg/L) were freshly prepared diluting methanolic PFAS stock solution with laboratory phase A and injected before each analytical batch. Regression equations of calibration curves were linear in the range of 2.5-0.01 or 0.05 or 0.1 µg/L depending on the analyte (see Table S5, LOQ). The results are expressed as the mean of 2 ± SD. Laboratory drinking water was checked for PFAS contamination: no PFAS were detected above LOD value.

Table S2: Elution gradients used for PFAS analyses. Mobile phases: (A) MeOH:aqueous NH_4OAc 2 mM 95:5; (B) NH_4OAc 2 mM in MeOH.

Time (min)	Flow (mL/min)	%A	%B
0.00	0.300	100.0	0.0
1.00	0.300	80.0	20.0
6.00	0.300	55.0	45.0
13.00	0.300	20.0	80.0
15.00	0.350	5.0	95.0
17.00	0.350	5.0	95.0
18.00	0.300	100.0	0.0
21.00	0.300	100.0	0.0

Table S3: Elution gradients used for PFOA analyses. Mobile phases: (A) MeOH:aqueous NH_4OAc 2 mM 95:5; (B) NH_4OAc 2 mM in MeOH.

Time (min)	Flow (mL/min)	%A	%B
0.00	0.300	70.0	30.0
5.00	0.300	5.0	95.0
7.00	0.300	5.0	95.0
8.00	0.300	70.0	30.0
11.00	0.300	70.0	30.0

Table S4: LC-MS/MS parameters for all PFAS target analytes using UPLC-MS/MS Waters ACQUITY UPLC H-Class PLUS – XEVO TQS Micro mass detector.

Name		**Monitored transition (ES^-)**	**Collision energy (eV)**	**LOQ µg/L)**
PFBA	Perfluorobutanoic acid	212.97→168.99	8	0.01
PFPeA	Perfluoropentanoic acid	263.09→218.93	6	0.01
PFBS	Perfluorohexanoic acid	299.03→79.84	32	0.01
PFHxA	Perfluoroheptanoic acid	312.90→269.02	6	0.01
PFHpA	Perfluorooctanoic acid	262.90→168.98	6	0.01
PFHxS	Perfluorononanoic acid	398.96→79.90	38	0.01
PFOA	Perfluorodecanoic acid	412.98→168.98	18	0.01
PFNA	Perfluoroundecanoic acid	462.96→218.97	16	0.01
PFOS	Perfluorododecanoic acid	498.90→79.90	54	0.01
PFDA	Perfluorotridecanoic acid	513.12→469.00	10	0.01
PFUnDA	Perfluorotetradecanoic acid	562.96→519.06	10	0.05
PFDODA	Perfluorobutanesulfonic acid	613.06→569.04	14	0.05
PFTrDA	Perfluorohexanesulfonic acid	622.90→168.97	28	0.05
PFTA	Perfluorooctanesulfonic acid	712.96→168.96	32	0.1

5. Surface-enhanced Raman spectroscopy (SERS)

The preparation of the substrates for the SERS analysis was carried out according to the following steps: the Si/SiO_2 substrate was placed on a heating plate at 50 °C. Then 20 µL of the AuNPs solution (10.7 nM) were added by drop casting and, finally, 1˙200µL of the standard test or sample were added. The prepared substrates were analyzed by SERS using an InVia Renishaw microspectrometer equipped with a 532 nm point-based laser. The power density was set at 50 mW and an acquisition time of 1 s was employed for all measurements. 3˙000 points per substrate were measured and the 3˙000 spectra were averaged to give a single spectrum for each replica, using a program generated in MATLAB R2020a with our own code. The spectrum of AuNPs was used as a control and was subtracted in all the samples. Samples of treated water were analyzed in order to detect release of GO, using the methodology previously described [1]. This method allows the quantification of GO nanosheets in water using surface-enhanced Raman spectroscopy (SERS). The intensity of the D-band is used as analytical signal (Fig. S6) and correlated with the concentration to

obtain a calibration curve in the range 0.1-10.0µg/L. The characteristic G band of GO cannot be used as analytical signal because of the interferences with the gold nanoparticle signal. No peaks around 1˙350 cm^{-1} were found in the Raman spectrum of PSU (Fig. S7) and no interferences are observed. The practical limit of quantification of this methodology was 0.1µg/L. This value is defined as the minimum amount of GO that can be measured with accuracy higher than 80% and relative standard deviation lower than 10%. Three replicates were carried out for each analyzed sample. Moreover, the relative standard deviation of the intensity values was calculated, for each sample (Fig. S8 and Table S2).

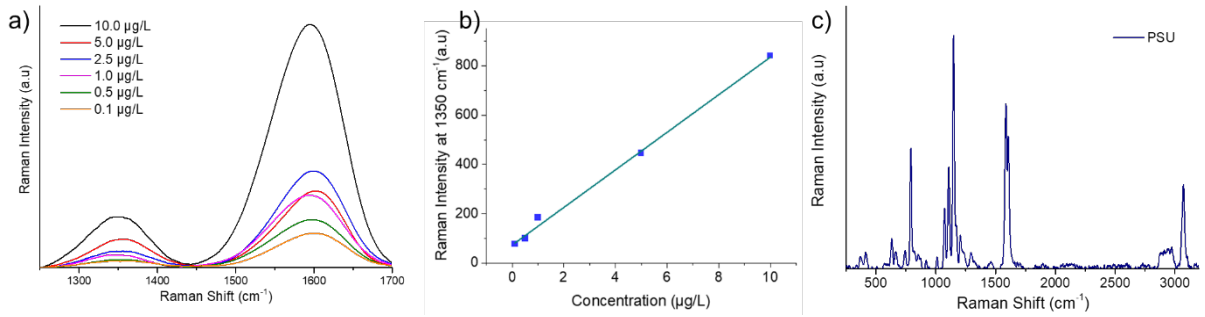

Fig. S6. a) SERS spectra of different GO concentrations in the range of 0.1–10 ⍰g L^{-1}, b) calibration curve, c) Raman spectrum of PSU.

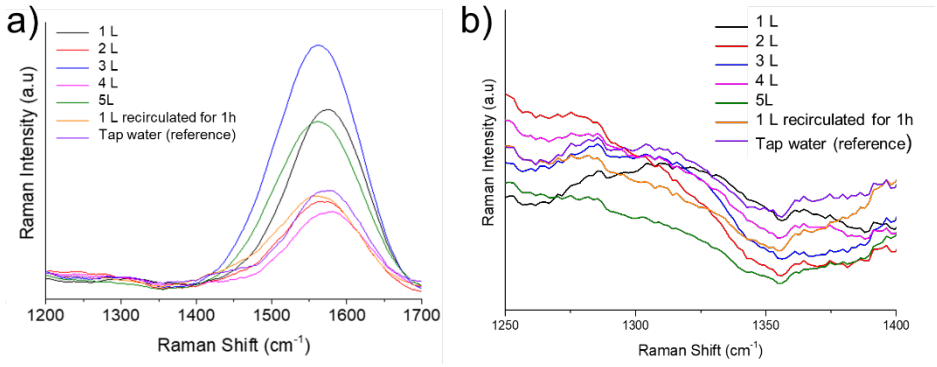

Fig. S7. a) SERS spectra of filtered water, from 1 L to 5 L, 1 L recirculated for 1 h, and tap water, b) Zoom at 1˙350 cm^{-1} of SERS spectra.

Table S5. Filtered water samples and intensity values (1˙350 cm^{-1}) measured on SERS substrates. Relative standard deviation (RSD) of intensity values (3˙000 points per sample) and obtained GO concentration (µg/L)

Sample	**Intensity (A.U.)**	**%Rsd**	**Concentration (µg/L)**
1 L	18.20	4.03	<0.1
2 L	12.30	5.28	<0.1
3 L	14.12	5.02	<0.1
4 L	15.98	4.97	<0.1
5 L	11.12	7.86	<0.1
1 L recirculate for 1h	14.37	3.63	<0.1
TAP water (reference)	17.64	8.22	-

6. Characterization

Optical microscopy. Optical microscopy was performed using a Nikon DS-2Mv digital camera, mounted on a Nikon Eclipse 80i optical microscope (Nikon, Melville, NY, USA).

Scanning electron microscopy (SEM). Scanning electron microscopy (SEM) analyses were acquired with ZEISS LEO 1530 FEG. The energy of electrons was 5 keV and inLens detector at a working distance of 3-5 mm acquired the signal.

Attenuated total reflection Fourier-transform infrared (ATR FT-IR). Attenuated total reflection Fourier-transform infrared (ATR FT-IR) spectra were recorded with Agilent Cary 630 FTIR spectrophotometer and the spectra are expressed by wavenumber (cm^{-1}).

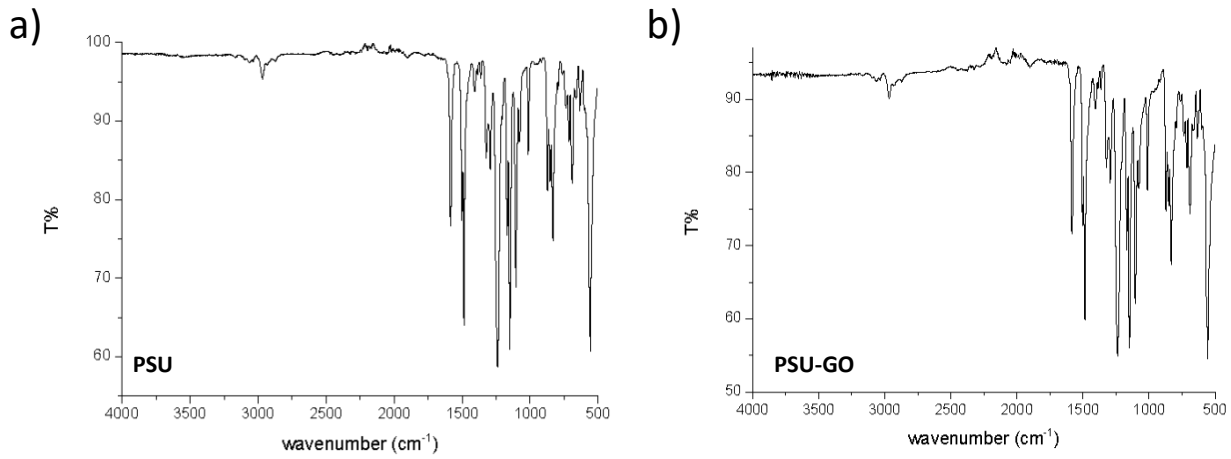

Fig. S8. Infrared Analysis on a) PSU and b) PSU-GO samples.

Thermogravimetric Analysis (TGA). Thermogravimetric analysis (TGA) has been investigated using a PerkinElmer TGA4000 apparatus in air atmosphere, from 30 °C to 800 °C, with a scanning temperature of 10 °C/min.

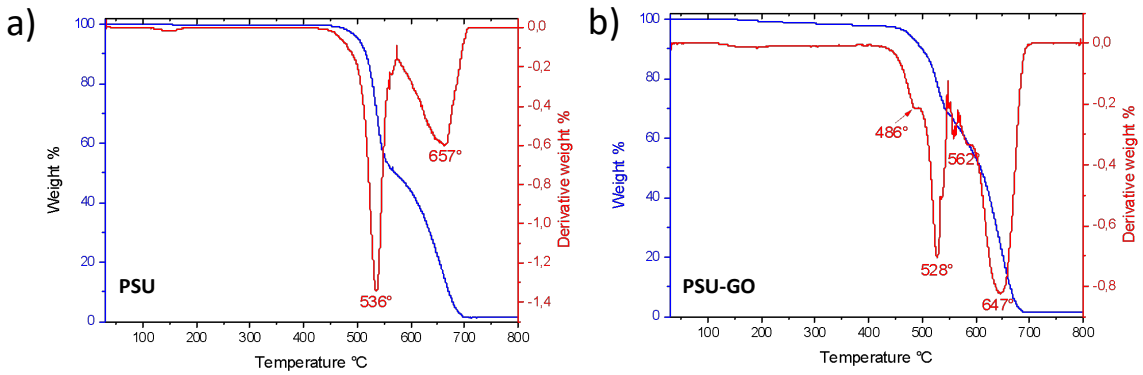

Fig. S9. Thermogravimetric analysis (TGA) on a) PSU and b) PSUGO samples.

7. Adsorption selectivity and mechanism

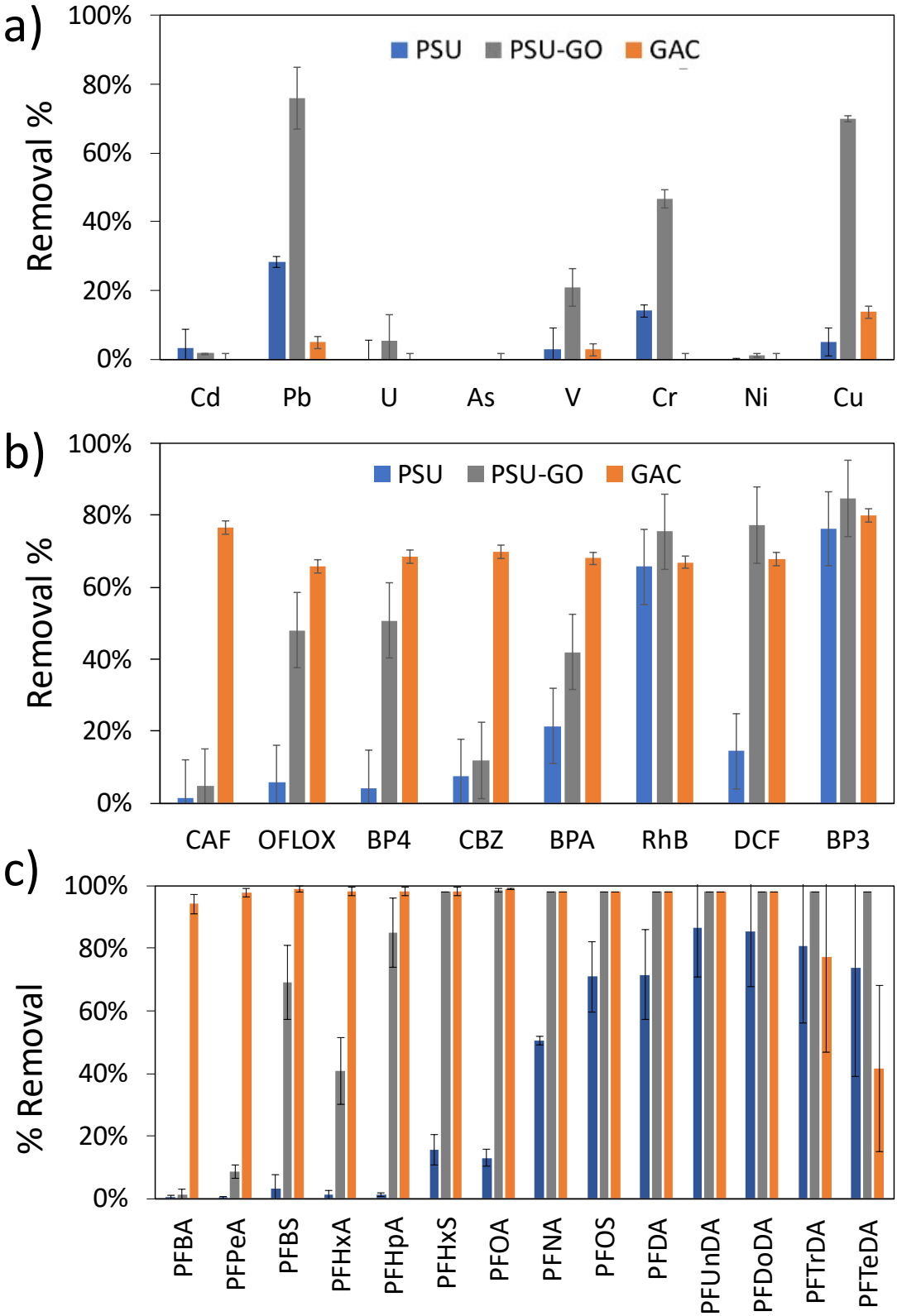

Fig. S10. Adsorption selectivity of cartridge of PSU (0.4g) PSU-GO (0.73g) and GAC (2.3g) towards mixture in tap water (flow rate = 20 mL/min, EBCT = 0.5 min, total treated volume 1 L, 100 bed volumes) of a) metals (C_{IN} = 100 µg/L each), b) selected organic contaminants (C_{IN} = 0.5 mg/L each), c) PFAS (C_{IN} = 0.5 µg/L each). PSU (blue bars), PSU-GO (grey bars) and GAC (orange bars) cartridge.

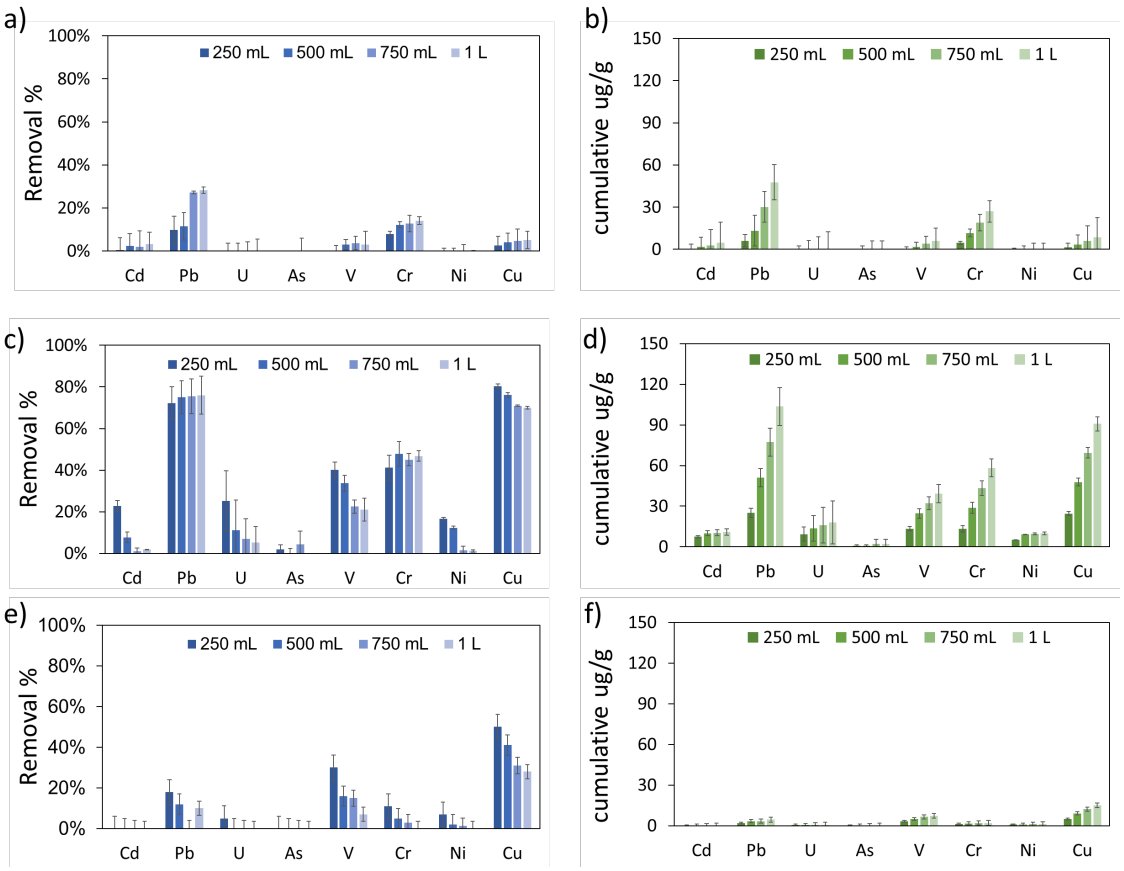

Fig. S11. Removal of a) PSU, c) PSU-GO, and e) GAC on a mixture of eight heavy metals and metalloids in tap water. Cumulative µg removed/g of b) PSU, d) PSU-GO and f) GAC. (C_{IN} = 100 µg/L each, V_{TOT} = 1 L, flow rate = 20 mL/min, EBCT = 0.5 min, bed volume=0.01 L)

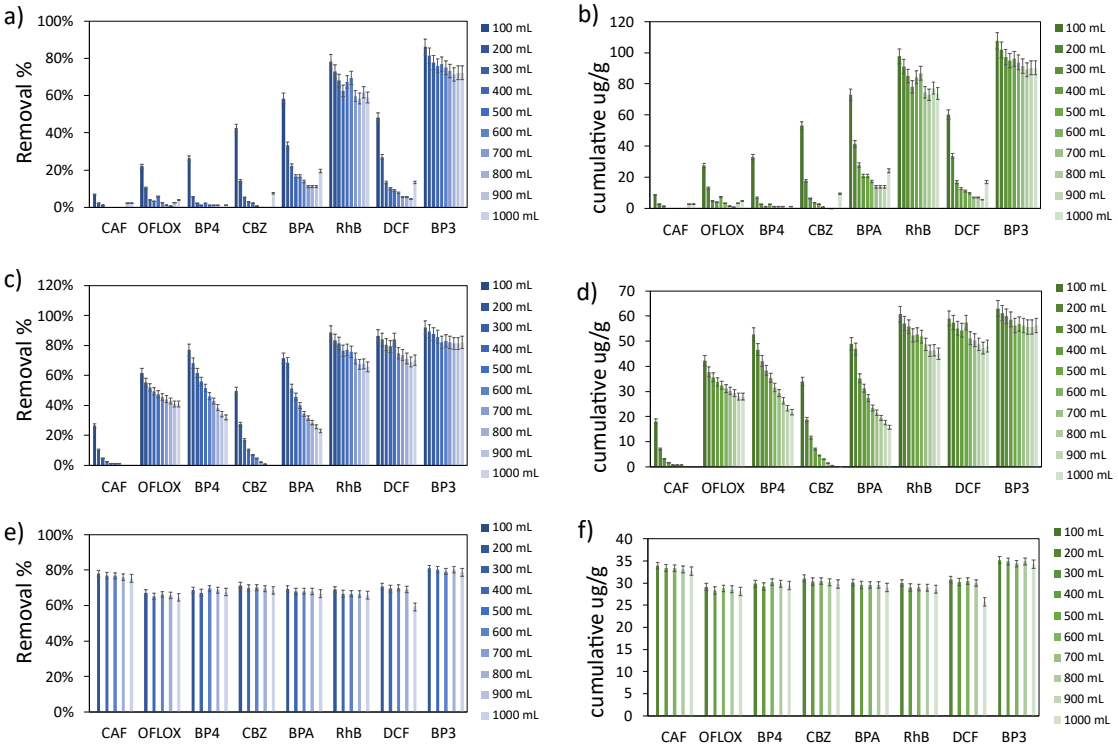

Fig. S12 Removal of a) PSU, c) PSU-GO, and e) GAC on a mixture of eight organic contaminants in tap water. Cumulativeµg removed/g of b) PSU, d) PSU-GO and f) GAC. (C_{IN} = 0.5 mg/L each, V_{TOT} = 1 L, flow rate = 20 mL/min, EBCT = 0.5 min, bed volume=0.01 L).

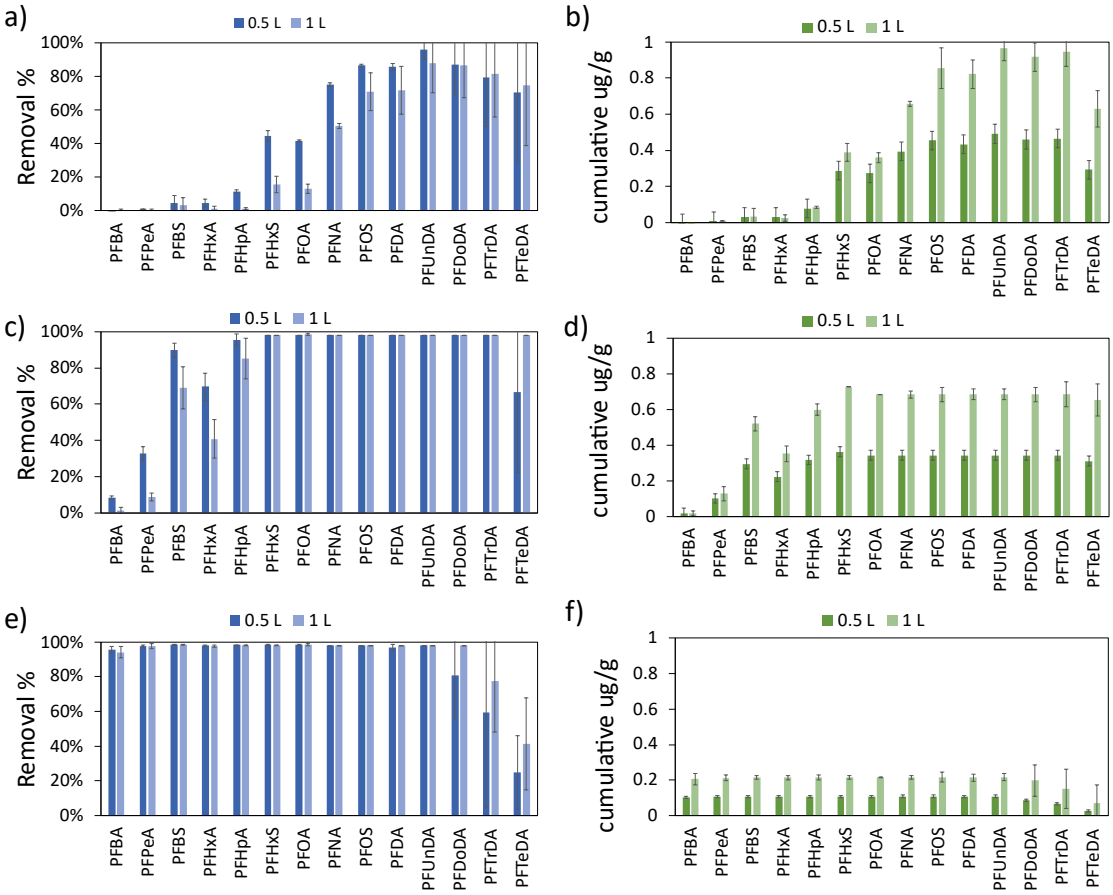

Fig. S13. Removal of a) PSU, b) PSU-GO and c) GAC on a mixture of fourteen PFAS in tap water. Cumulative µg removed/g of b) PSU, d) PSU-GO and f) GAC. (C_{IN} = 0.5 µg/L each, V_{TOT} = 1 L, flow rate = 20 mL/min, EBCT = 0.5 min, bed volume=0.01 L).

Table S6. n-Octanol/water partition coefficient ($logK_{ow}$) of carboxylic PFAS, and removal for PSU and PSU-GO.

	Log K_{ow}	PSU		PSU-GO	
		µg/g	Removal %	µg/g	Removal %
PFBA (CF_3)	2.31[2]	0.001	0	0.017	1
PFPeA (CF_4)	3.01[2]	0.007	0	0.128	9
PFHxA (CF_5)	3.48[2]	0.024	1	0.352	41
PFHpA (CF_6)	4.15[2]	0.085	1	0.600	85
PFOA (CF_7)	4.81[2]	0.359	13	0.683	98
PFNA (CF_8)	5.48[2]	0.657	51	0.685	98
PFDA (CF_9)	6.51[2]	0.822	72	0.685	98
PFUnDA (CF_{10})	7.20[2]	0.967	88	0.685	98
PFDoDA (CF_{11})	7.92[2]	0.918	86	0.685	98
PFTrDA (CF_{12})	8.62[2]	0.946	82	0.685	98
PFTeDA (CF_{13})	9.32[2]	0.630	75	0.652	98

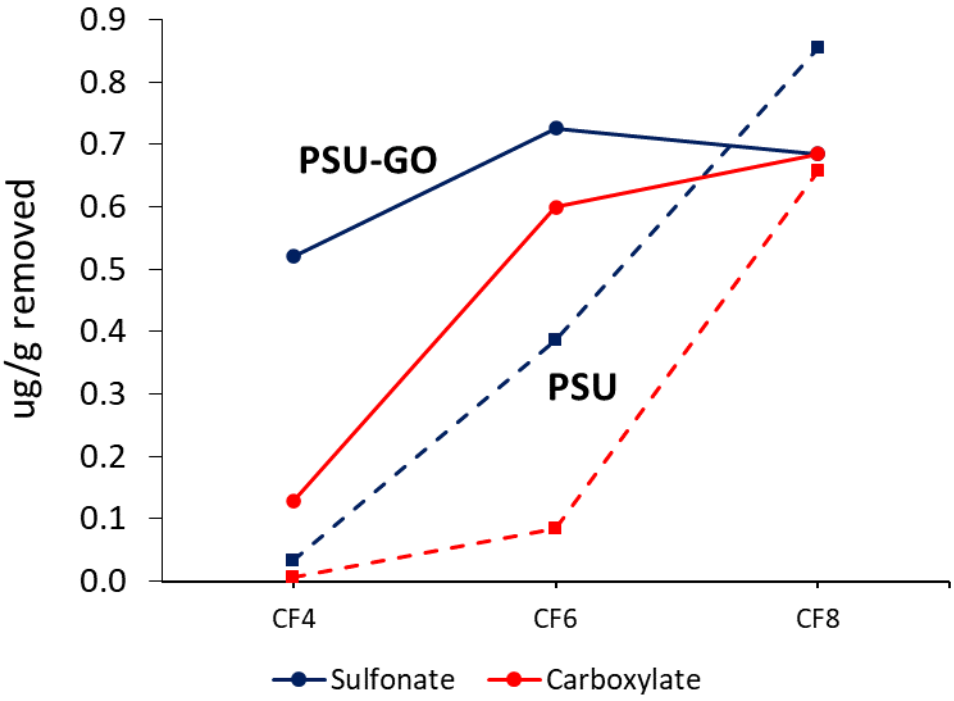

Fig. S14. Comparison between the mg of PFAS/g removed by PSU-GO (solid line) and PSU (dotted line). The µg removed of sulfonate (blue) and carboxylate (red) PFAS have been correlated to the number of fluorinated carbon (CF_n).

Table S7. Comparison between the removal of sulfonate and carboxylate PFAS correlated to the number of fluorinated carbon (CF_n) and K_{ow}.

	Log K_{ow}	PSU		PSU-GO	
		µg/g	Removal %	µg/g	Removal %
PFBA (CF_3)	1.82[2]	0.03	3	0.52	69
PFPeA (CF_4)	3.01[2]	0.01	0	0.13	9
PFHxA (CF_5)	3.16[2]	0.39	16	0.73	98
PFHpA (CF_6)	4.15[2]	0.09	1	0.60	85
PFOA (CF_7)	4.49[2]	0.85	71	0.68	98
PFNA (CF_8)	5.48[2]	0.66	51	0.68	98

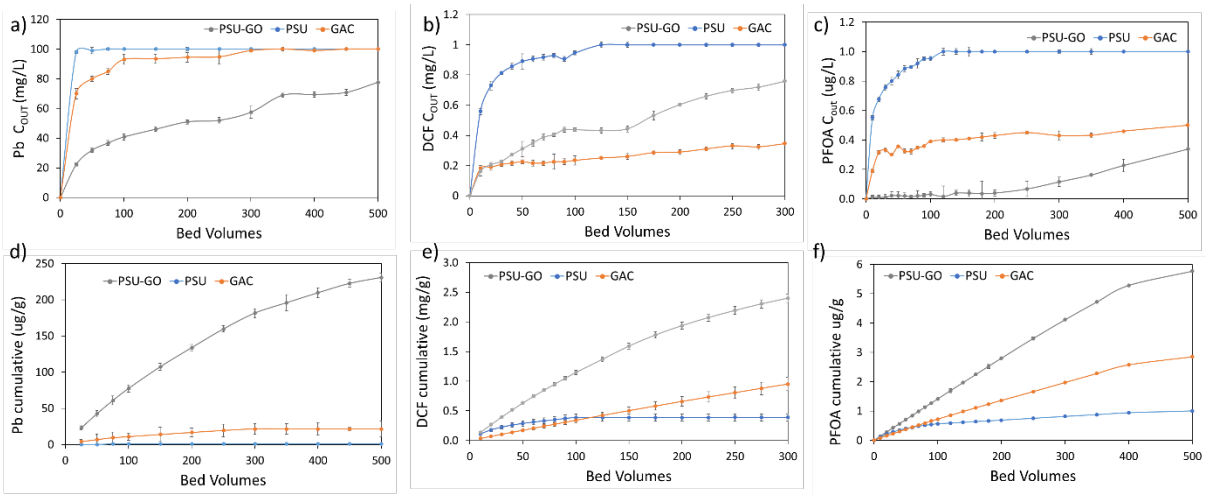

Fig. S15. Loading curve of a) Pb , b) DCF, c) PFOA, ,cumulative mg/g removed for d) Pb, e) DCF and f) PFOA Results are expressed in Bed Volumes (Vol treated/V cartridge).

.

The breakthrough point as been identified for $C_{OUT}=C_{IN}$, meaning that the cartridge is no more able to absorb contaminants. This point is particular evident in the figure a), b), c).

In the case of Pb, the breakthrough point was reached after 25 bed volumes for PSU and at 300 bed volumes for GAC, while PSU-GO never reach saturation.

In the case of DCF, breakthrough point was reached by PSU after 125 bed volumes, while PSU-GO and GAC never reach saturation. With PFOA, breaktrought point was identified at 120 bed volumes for PSU, while in the range of Volumes treated, GAC and PSU-GO never reached breaktrought.

8. Molecular dynamic modelling

The generalized AMBER force field (GAFF) [3] was used to parameterize PFAS molecules. Atomic charges were calculated at HF/6-31G(d) level, followed by restrained electrostatic potential (RESP) fitting. The model-systems representing GO was modelled on a 40 Å x 40 Å graphene sheet created with visual molecular dynamics (VMD) [4]. The epoxy, hydroxyl, carbonyl, and carboxylic acid groups were randomly positioned on graphene sheet to reproduce the experimental XPS data. The GAFF force field was also used to describe GO. In this case, the atomic charges were obtained by AM1 calculations. Each PFAS/GO complex was inserted into a box of TIP3P water molecules and counterions were added to neutralize the total charge. The resulting systems were minimized using a two-steps procedure employing Amber16 [5]. First, harmonic constraints (500 kcal mol^{-1} $Å^{-2}$) on the PFAS/GO complex, relaxing only the position of waters molecules and ions. Second, all the system is free to move. The resulting minimized structures were used as starting points for molecular dynamics simulations. An equilibration step of 10 ns was carried out gradually heating the system from 0 to 298 K, using an Andersen thermostat and periodic boundary conditions (PBC). Then 100 ns of molecular dynamics simulations were carried out (production runs). Molecular mechanics – generalized Born surface area (MM-GBSA) calculations were carried out to compute the binding affinity of PFAS to GO. For each calculation, 5˙000 frames were used, extracting the snapshots from the MD trajectories.

9. Release, regeneration and reuse experiments

The release of adsorbed molecules from the cartridge was studied flowing 1 L of fresh tap water in saturated cartridge at 20 mL/min. The final concentration of DCF, PFOA, and Pb in filtered water was analyzed by UV–Vis, UPLC-MS/MS, and ICP-MS analyses, respectively.

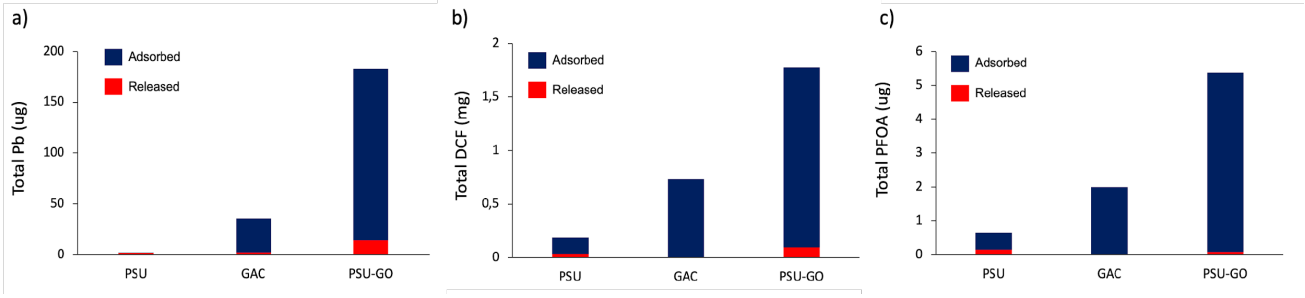

Fig. S16. Release of a) Pb, b) DCF, and c) PFOA for saturated PSU, PSU-GO, and GAC cartridge with tap water.

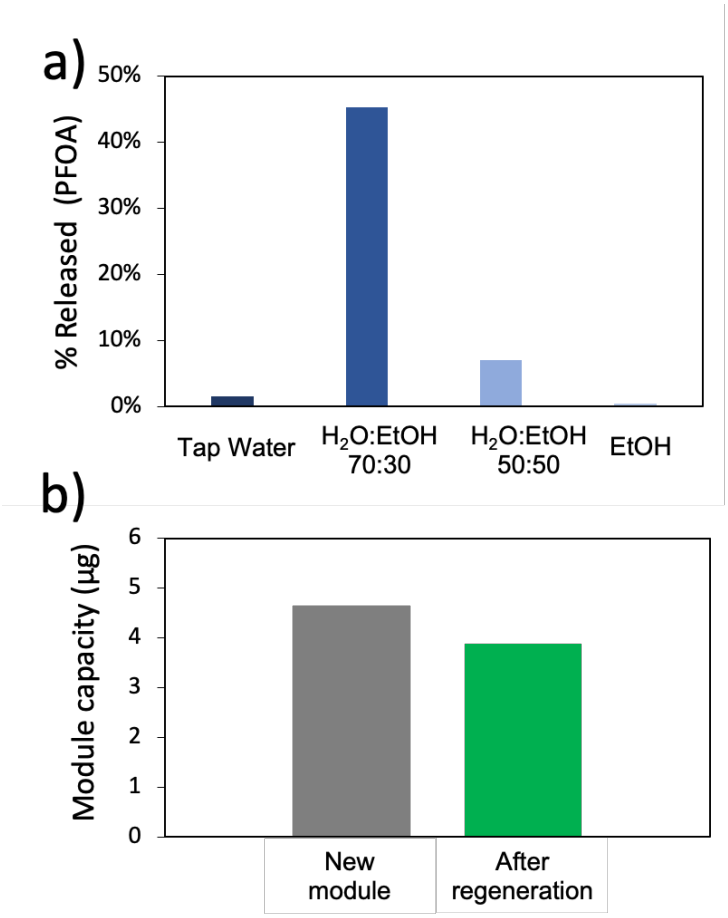

Figure S17. a) Release of PFOA for PSU-GO washed with different ultrapure water: EtOH mixtures and b) mg of PFOA adsorbed by a cartridge before and after regeneration.

10. Potability test

Parameter *Method*	PSU-GO	Limits
Turbidity *APAT CNR IRSA 2110 Man 29 2003*	<0.02	
Smell *APAT CNR IRSA 2050 Man 29 2003*	Odorless	
Taste	Tasteless	

APAT CNR IRSA 2080 Man 29 2003			
Color	Colorless		
APAT CNR IRSA 2020 A Man 29 2003			
pH	8	*±0.4*	6.5/9.5
APAT CNR IRSA 2060 Man 29 2003			
TOC (mg/L)	< 1		
UNI EN 1484:1999			
Conductivity (microS/cm)	508	*±38*	<2500
APAT CNR IRSA 2030 Man 29 2003			
Water hardness (°F)	55	*±11*	15/50
APAT CNR IRSA 3010 B			
+ APAT CNR IRSA 3020 Man 29 2003			
Fixed residue a 180°C (mg/L)	389.0	*±31.1*	<1500
APAT CNR IRSA 2090 B Man 29 2003			
Ammoniacal nitrogen$^{(NH4+)}$ (mg/L)	<0.02		
UNI 11669:2017			
Chloride (mg/L)	38.50	*±3.85*	<250
APAT CNR IRSA 4020 Man 29 2003			
Sulphate (mg/L)	117.1	*±14.1*	<250
APAT CNR IRSA 4020 Man 29 2003			
Nitrite (mg/L)	0.07	*±0.01*	<0.5
APAT CNR IRSA 4020 Man 29 2003			
Iron (ICP-MS) (µg/L)	9.2	*±0.8*	<200
EPA 6020B 2014			
Aluminium (ICP-MS) (µg/L)	7.6	*±0.7*	<200
EPA 6020B 2014			
Manganese (ICP-MS) (µg/L)	<0.1		<50
EPA 6020B 2014			
Sodium (mg/L)	38.81	*±5.59*	<200
APAT CNR IRSA 3010 B			
+ APAT CNR IRSA 3020 Man 29 2003			
Escherichia coli	0		<0
UNI EN ISO 9308-1:2017			
Intestinal Enterococci	0		<0
UNI EN ISO 7899-2:2003			
Antimony (ICP-MS) (µg/L)	<0.1		<0.5
EPA 6020B 2014			
Arsenic (ICP-MS) (µg/L)	<0.1		<10

EPA 6020B 2014			
Boron (mg/L)	0.12	*±0.02*	
APAT CNR IRSA 3010 B + APAT CNR IRSA 3020 Man 29 2003			
Cadmium (ICP-MS) (µg/L)	0.01	*±0.002*	<5.0
EPA 6020B 2014			
Chromium (ICP-MS) (µg/L)	0.6	*±0.09*	<50
EPA 6020B 2014			
Mercury (ICP-MS) (µg/L)	<0.1		<1.0
EPA 6020B 2014			
Nichel (ICP-MS) (µg/L)	0.5	*±0.07*	<20
EPA 6020B 2014			
Lead (ICP-MS) (µg/L)	0.5	*±0.07*	<10
EPA 6020B 2014			
Copper (mg/L)	<0.01		
APAT CNR IRSA 3010 B + APAT CNR IRSA 3020 Man 29 2003			
Selenium (mg/L)	<0.06		
APAT CNR IRSA 3010 B + APAT CNR IRSA 3020 Man 29 2003			
Vanadium (ICP-MS) (µg/L)	0.3	*±0.04*	<50
EPA 6020B 2014			
1.2-Dichloroethane (µg/L)	<0.1		
EPA 5030C 2003 + EPA 8260D 2018			
Fluorides (mg/L)	0.09	*±0.02*	
APAT CNR IRSA 4020 Man 29 2003			
Nitrate (mg/L)	3.21	*±0.48*	<50
APAT CNR IRSA 4020 Man 29 2003			
Nitrite (mg/L)	0.07	*±0.01*	<0.5
APAT CNR IRSA 4020 Man 29 2003			
Trihalomethanes (Total) (µg/L)	<0.05		
EPA 5030C 2003 + EPA 8260D 2018			
Vinyl chloride (µg/L)	<0.1		
EPA 5030C 2003 + EPA 8260D 2018			
Chlorites (µg/L)	<0.1		
APAT CNR IRSA 4020 Man 29 2003			
Benzo(a)pyrene (µg/L)	<0.002		
APAT CNR IRSA 4020 Man 29 2003			
Benzene (µg/L)	<0.1		
EPA 5030C 2003 + EPA 8260D 2018			
Acrylamide (µg/L)	<0.01		

EPA 5030C 2003 + EPA 8260D 2018		
Brominated (mg/L)	<0.1	
APAT CNR IRSA 4020 Man 29 2003		
Free Cyanides (µg/L)	<0.05	
APAT CNR IRSA 4020 Man 29 2003		
Polycyclic Aromatic Hydrocarbons (µg/L)	<0.002	
EPA 8272 2007		
Total Pesticide (µg/L)	<0.02	
APAT CNR IRSA 4020 Man 29 2003		
Epichlorohydrin (µg/L)	<0.1	
EPA 5030C 2003 + EPA 8260D 2018		
Tetrachloroethylene + trichloroethylene (µg/L)	<0.1	
EPA 5030C 2003 + EPA 8260D 2018		

11. Experiments on mechanical grinded PSU-GO granules (Pilot plant testing-standard sized commercial cartridges)

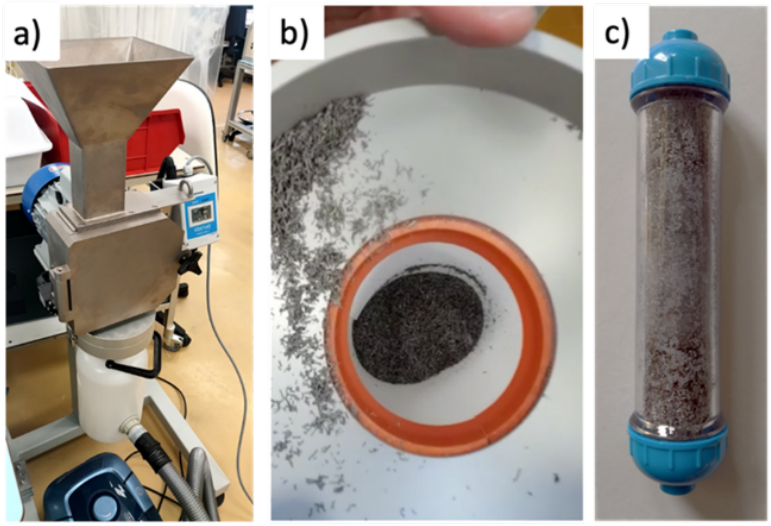

Fig. S18 a) Mechanical blade grinder, b) zoom of PSU-GO granules obtained, c) larger cartridge filled with the obtained granules (49 mm diameter, 250 mm length, EBCT = 0.14 min, bed volume = 0.5 L) of PSU-GO,

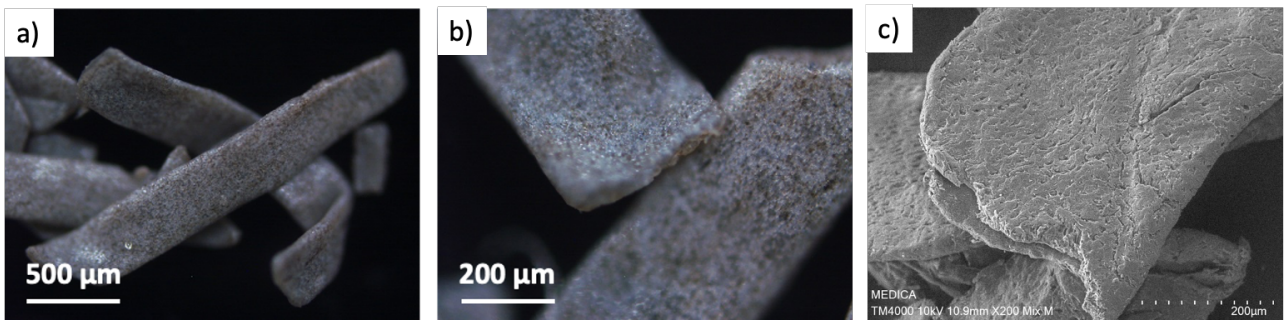

Fig. S19. a, b) Optical microscopy images at different magnification and c) SEM image of granules obtained by mechanical grinding of scraps of PSU-GO-HF.

Release test of chromium from PSU-GO and PSU granules. We studied the release of Cr in water from PSU and PSU-GO granules to exclude a significant presence of chromium caused by the blades during the grinding. 1 g of unwashed PSU granules was stirred in 200 mL of tap water for 3 days, then filtered on a mixed cellulose esters filter (cut-off 0.22 mm) to separate the granules from the aqueous phase. The latter was immediately acidified with 1% NHO_3 and analysed with an ICP-MS (details in SI, section 5.1). The same procedure was performed on 1 g of PSU-GO granules.

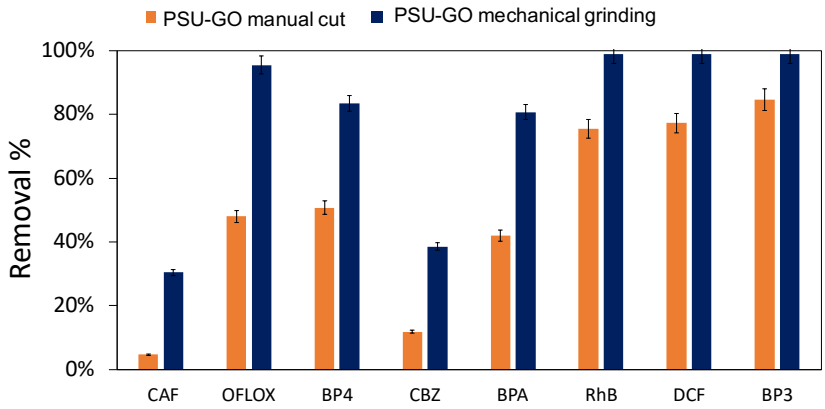

Fig. S20. Comparison of the adsorption of manually grinded PSU-GO and mechanically grinded PSU-GO. Small cartridge (Fig. S3) filled by 0.7 g of material were used. Tap water solution (1 L), 0.5 mg/L each contaminant, flow rate = 20 mL/min, EBCT= 0.5 min, bed volumes= 0,01 L.

12. Pilot plant working conditions

As shown in Fig. 6a, the system comprises two tanks with a capacity of 100 L each (Namely tank "1", on the left, and tank "2" on the right) allowing water circulation (with the chance of by-passing the filter under test), and it is connected to the tap with a pump driving water into the first tank. Pressurization is controlled by a valve, and the inlet pressure was maintained at a constant 2 bars to represent average tap pressure.

The pilot system includes flow rate measurement and the capability to program start-stop cycles with real-time monitoring of pressure, flow rate, and partial/total volume. During the experiments, Tank 1 is filled with spiked tap-water, which is then pumped through the filtering cartridge. A new cartridge was used for each contaminant. After the cartridge, a tap allows for the collection of filtered water samples at predefined intervals for further analyses and quantification. The remaining water is then collected in tank 2. After treating 100 L, the maximum capacity of the tanks, water can be re-pumped into the first tank, by-passing the cartridge, to recycle the contaminated water. The concentration of the contaminant is then quantified and re-adjusted to ensure constant initial concentration during all the experiment.

The advantage of using the pilot plant with respect to the direct Point of Use testing is that it allows for water recharge and recycle, thus it allows us to test the cartridges on thousand liters of water without producing large volume of contaminated water to be then disposed.

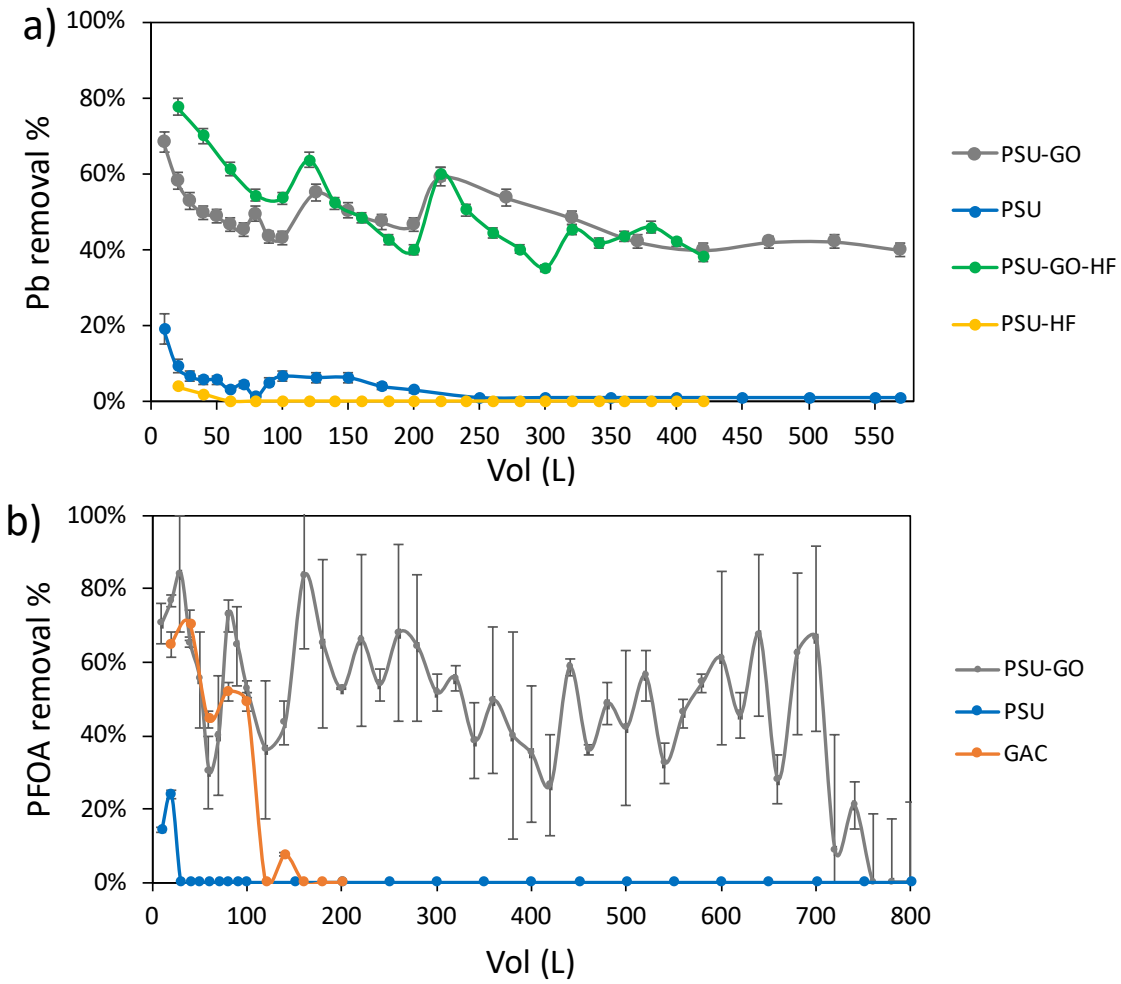

Fig. S21. Comparison between removal capacity of tested cartridge on a) Pb and b) PFOA.

13. References:

1. E. Briñas, V. J. González, M. A. Herrero, M. Zougagh, Á. Ríos and E. Vázquez, *SERS-Based Methodology for the Quantification of Ultratrace Graphene Oxide in Water Samples*, *Environ. Sci. Technol.*, 2022, **56**, 9527-9535, https://doi.org/10.1021/acs.est.2c00937
2. E. Gagliano, M. Sgroi, P. P. Falciglia, F. G. A. Vagliasindi and P. Roccaro, *Removal of poly- and perfluoroalkyl substances (PFAS) from water by adsorption: Role of PFAS chain length, effect of organic matter and challenges in adsorbent regeneration*, *Water Res.*, 2020, **171**, 115381, https://www.sciencedirect.com/science/article/pii/S0043135419311558
3. J. Wang, R. M. Wolf, J. W. Caldwell, P. A. Kollman and D. A. Case, *Development and testing of a general amber force field*, *J. Comput. Chem.*, 2004, **25**, 1157-1174, https://onlinelibrary.wiley.com/doi/abs/10.1002/jcc.20035
4. W. Humphrey, A. Dalke and K. Schulten, *VMD: Visual molecular dynamics*, *J. Mol. Graphics*, 1996, **14**, 33-38, https://www.sciencedirect.com/science/article/pii/0263785596000185
5. R. M. B. D.A. Case, D.S. Cerutti, T.E. Cheatham, III, T.A. Darden, R.E. Duke, T.J. Giese, H. Gohlke, A.W. Goetz, N. Homeyer, S. Izadi, P. Janowski, J. Kaus, A. Kovalenko, T.S. Lee, S. LeGrand, P. Li, C. Lin, T. Luchko, R. Luo, B. Madej, D. Mermelstein, K.M. Merz, G. Monard, H. Nguyen, H.T. Nguyen, I. Omelyan, A. Onufriev, D.R. Roe, A. Roitberg, C. Sagui, C.L. Simmerling, W.M. Botello-Smith, J. Swails, R.C. Walker, J. Wang, R.M. Wolf, X. Wu, L. Xiao and P.A. Kollman, *AMBER*, University of California, San Francisco., 2016.